

---

# CERTIFIED HUMAN TRAJECTORY PREDICTION

---

Mohammadhossein Bahari<sup>\*,1</sup>

Saeed Saadatnejad<sup>\*,1</sup>

Amirhossein Asgari Farsangi<sup>1</sup>

Seyed-Mohsen Moosavi-Dezfooli<sup>2</sup>

Alexandre Alahi<sup>1</sup>

<sup>1</sup>EPFL, <sup>2</sup>Imperial College London

{mohammadhossein.bahari, saeed.saadatnejad}@epfl.ch

## ABSTRACT

Trajectory prediction plays an essential role in autonomous vehicles. While numerous strategies have been developed to enhance the robustness of trajectory prediction models, these methods are predominantly heuristic and do not offer guaranteed robustness against adversarial attacks and noisy observations. In this work, we propose a certification approach tailored for the task of trajectory prediction. To this end, we address the inherent challenges associated with trajectory prediction, including unbounded outputs, and multi-modality, resulting in a model that provides guaranteed robustness. Furthermore, we integrate a denoiser into our method to further improve the performance. Through comprehensive evaluations, we demonstrate the effectiveness of the proposed technique across various baselines and using standard trajectory prediction datasets. The code will be made available online: <https://s-attack.github.io/>

## 1 Introduction

Predicting the behavior of humans is a crucial task for the safe operation of an autonomous vehicle. The task is known as human trajectory prediction and aims to predict the future positions of humans using their past positions as input data. Trajectory prediction has received significant attention, and the recent data-driven methodologies have exhibited remarkable performance [20, 45]. Despite these advancements, it has been shown that these methods are susceptible to adversarial attacks raising significant robustness and security concerns [36, 9, 41]. Moreover, recent findings indicate that integrating prediction models in real-world autonomous driving pipelines results in a drastically lower performance [46], due to the noises coming from the upstream modules (*e.g.*, detection and tracking) which are posed into the inputs of the prediction model. This vulnerability of the prediction models to input noise, further underscores the need for enhancing their robustness.

Previous works proposed heuristic approaches to enhance the robustness of the trajectory prediction models [50, 10, 25]. While these approaches have achieved enhanced robustness, they fall short of providing guaranteed robustness. It has been shown that such heuristic approaches are ultimately ineffective against sufficiently powerful adversaries [12, 42, 2]. Therefore, it is essential to study approaches that provide *guaranteed* robustness.

Certification is a line of research that provides guaranteed robustness against input noise such as adversarial attacks. Among the existing certification techniques, “Randomized Smoothing” [15] stands out as a widely-used approach because of its simplicity, model-agnostic nature and computational efficiency. More importantly, it imposes the least assumptions on the input noise distribution, providing robustness against any bounded noise, including adversarial attacks. Randomized smoothing transforms a base model into a smoothed model by adding random perturbations to the input, and then aggregating the outputs to give the most probable output. The key feature of the smoothed model is that its outputs are certified as long as the input noise is within the certification radius.

In this paper, we introduce a method based on randomized smoothing certification for trajectory prediction models, which delivers guaranteed robustness by providing guaranteed output bounds. As depicted in Figure 1, even slight perturbations in observation inputs can lead to considerably different predictions. Nevertheless, predictions from

---

\* Equal contribution.

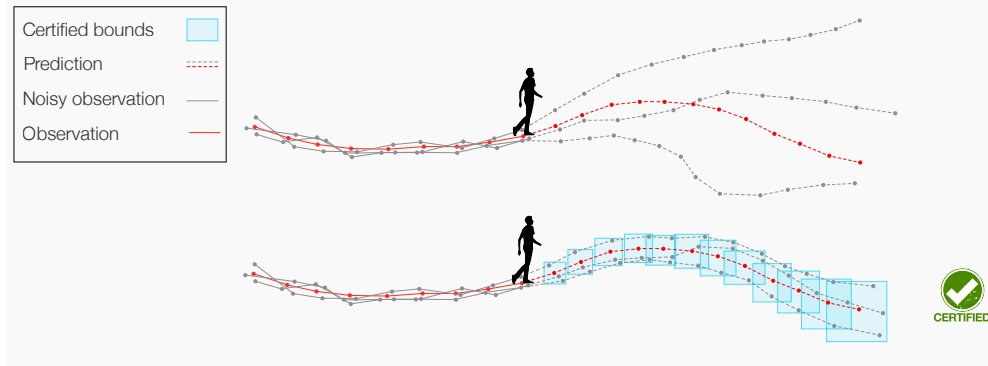


Figure 1: Illustration of the influence of noisy inputs on trajectory prediction models. The noise can stem from an adversarial attack, or errors of the upstream modules (*e.g.*, detection). The red trajectories depict clean observations and the corresponding predictions, and the gray trajectories represent predictions with noisy inputs. The top part showcases the outputs of an original trajectory prediction model, revealing unbounded predictions. In contrast, the bottom part demonstrates the outputs of our trajectory predictor with certified robustness, underscoring our ability to guarantee bounds on predicted outputs. This model is robust against adversarial attacks and is more reliable due to the guaranteed bounds.

our model with certified robustness invariably stay within its guaranteed bounds. Given the black-box nature of the prediction models, the bounds of the outputs deliver reliability to the system which is crucial for autonomous vehicles.

Up to our knowledge, we are the first to study the application of randomized smoothing in trajectory prediction models, encountering various challenges. (1) How can we transform the randomized smoothing technique widely applied in image classification, to the multi-output regression task of trajectory prediction and what is the suitable aggregator? (2) While randomized smoothing hurts performance considerably in the classification task, to what extent it hurts the accuracy of trajectory prediction models and is there a way to maintain the accuracy? (3) Unlike the tasks addressed in prior works, trajectory prediction is a time-series regression task that does not inherently pose a maximum output range, which is essential for the randomized smoothing algorithm. How can we pose a range for the outputs? (4) Finally, rather than one output, trajectory prediction models are often multi-modal, generating multiple output modes. Therefore, a new definition for certification is required that can accommodate multi-modal outputs. In order to address the aforementioned challenges, (1) we adapt two randomized smoothing approaches based on mean [15] and median [14] aggregation functions to trajectory prediction and compare their performances. (2) To mitigate the performance degradation resulting from randomized smoothing, we integrate a denoiser which is particularly effective for trajectory data fed into the smoothed model. (3) We also propose an adaptive clamping strategy to pose maximum output ranges. (4) Finally, we address the multi-modality challenge by proposing a new certification definition considering the best output mode among the outputs.

We conduct experiments employing state-of-the-art trajectory prediction models trained on Trajnet++ benchmark [26]. We demonstrate the accuracy and the certified output bound of the smoothed models and show their trade-off. We also showcase the robustness of the smoothed model against different inputs. We further reveal that common performance metrics are unreliable as they do not account for the potential input noises so we introduce new certified metrics, equipped with the certified bounds. At the end, we compare the performance of different denoisers, and investigate the impact of employing the denoiser in the smoothed model performance.

In summary, our contributions are as follows:

- We introduce certification to the trajectory prediction task, providing guaranteed robustness for models against adversarial attacks and noisy inputs.
- We develop a randomized smoothed trajectory prediction method that yields accurate predictions, tailored to the unique aspects of the task, such as unbounded and multi-modal outputs.
- Through comprehensive experiments, we not only establish certified output bounds for various trajectory prediction baselines but also introduce new certified performance metrics.

## 2 Related Works

**Human trajectory prediction.** In recent years, as autonomous driving systems and social robots have become more popular, the challenge of predicting human trajectories has caught much attention. The majority of the research revolves around enhancing accuracy by learning the interaction dynamics between humans more effectively. To this end, Social-LSTM [1] is the pioneering work employing neural networks. Subsequent studies propose different architectural solutions based on Convolutional Neural Networks [33, 48], Graph Neural Networks [7, 32], and Transformers [21, 19, 37]. Additional approaches have incorporated the domain knowledge [27, 30], developed equivariant feature learning [20, 45] and explored various strategies for pooling social features [26, 3, 24]. In this work, we study the robustness of some of these models.

**Adversarial robustness for trajectory prediction.** The vulnerability of trajectory prediction models to adversarial attacks has been shown in several previous works [36, 9, 41]. To address this vulnerability, others proposed robustness defenses based on various heuristic approaches [36, 50, 10, 25]. However, none of these approaches are guaranteed robustness methods. Trajpac [49] is the pioneering work that proposed a guaranteed approach for the robustness of trajectory prediction models. They employ a probably approximately correct (PAC) strategy by approximating the prediction model locally with a linear model and use it as a proxy to determine the robustness of the model. However, their method has some limitations: (1) Their method is not agnostic to the input noise distribution due to the dependency of learned linear model on the noise distribution fed during learning. (2) Their method is inefficient in the number of required samples, with experiments often necessitating over 30,000 random samples. (3) Their method is probabilistic, and does not provide a guaranteed robustness. In this work, we employ a randomized smoothing approach that provides a guaranteed error bound, requires significantly fewer samples, and generalizes to any noise distribution encountered during deployment.

**Randomized smoothing certification.** Certification is to guarantee that a model’s outputs are within a bound around its initial output once the model’s inputs are within a neighborhood of its initial input and is mainly used as a defense against adversarial attacks. Various certification and verification methods have been proposed based on Satisfiability Modulo theories [17, 22], mixed integer linear programming [5, 18], solving optimization problems [44, 16] and layer by layer outer approximation of activations [40]. However, these methods are computationally expensive and are unable to scale to common neural networks. As an alternative, randomized smoothing has been proposed as an efficient and model-agnostic approach and has achieved great success in the classification task [8, 29, 11]. In randomized smoothing, the smoothed prediction for a given input is calculated by sampling some points around that input and aggregating their corresponding outputs. Certified output bounds for randomized smoothed models have been proven [15]. They prove a tight bound for these models with a mean aggregator, particularly for the classification task. Moreover, it was shown that integrating a denoiser into a randomized smoothed model can significantly enhance both accuracy and certification bounds [38]. Recently, randomized smoothing certification has been adapted for the detection task [14]. It introduces the use of a median smoothing aggregator which is more appropriate for regression tasks. To the best of our knowledge, our work is the first to propose randomized smoothing certification for the trajectory prediction problem, studying both mean and median smoothing.

Randomized smoothing is different from other methods that guarantee models’ output such as conformal prediction [39] since conformal prediction provides ground truth coverage guarantee rather than output region guarantee. Moreover, unlike randomized smoothing, conformal prediction is dependent on the input noise distribution (calibration set). Randomized smoothing is also different from uncertainty quantification approaches [23] in that they capture the uncertainty of the model or the task and do not consider the input noise.

## 3 Method

In this section, we first explain the certification approach, then the formulation of trajectory prediction and the details of our approach, followed by the algorithm.

### 3.1 Certification

Randomized smoothing [15] is a powerful technique initially introduced for certifying the robustness of machine learning models against  $\ell_2$ -norm adversarial attacks in image classification. In essence, given a prediction function  $f$  and an input certification radius  $R$ , randomized smoothing aims to bound the output of a smoothed function  $\tilde{f} = \mathcal{A}(f)$ , where  $\mathcal{A}$  is an aggregation/smoothing operator. Here, we consider two common choices for the smoothing operator: mean [15] and median [14] smoothing.

**Mean smoothing.** Given a function  $f : \mathbb{R}^d \rightarrow [l, u]$  with lower bound  $l$  and upper bound  $u$ , input  $X \in \mathbb{R}^d$ , and an input certification radius  $R$ , mean smoothing computes the expected value of the predictor over a perturbed input, that is

$$\tilde{f}(X) = \mathbb{E}_\epsilon[f(X + \epsilon)], \quad (1)$$

where  $\epsilon \sim N(0, \sigma^2 I)$ . It has been shown that for an input certification radius  $R$ ,  $\|r\|_2 < R$ , the output of  $\tilde{f}$  can be bounded as:

$$l + (u - l) \cdot \Phi\left(\frac{\eta(X) - R}{\sigma}\right) \leq \tilde{f}(X + r) \leq l + (u - l) \cdot \Phi\left(\frac{\eta(X) + R}{\sigma}\right), \quad (2)$$

where  $\eta(X) = \sigma \cdot \Phi^{-1}\left(\frac{\tilde{f}(X) - l}{u - l}\right)$  and  $\Phi$  is the cumulative distribution function of the standard Gaussian.

For a multi-output predictor  $f : \mathbb{R}^d \rightarrow [l_1, u_1] \times [l_2, u_2] \times [l_1, u_1] \times \dots \times [l_m, u_m]$ , where  $f(X) = (f_1(X), \dots, f_m(X))$ , the certification bounds are applicable individually to each coordinate. This setting is commonly encountered in trajectory prediction models. In [Section 3.2](#), we will provide a detailed explanation of the estimation process for  $l_i$ 's and  $u_i$ 's in our problem.

Note that this smoothing method is applicable to functions with initial lower and upper bounds. However, for functions that inherently lack those, an alternative option is to use median smoothing.

**Median smoothing.** Given a continuous function  $f : \mathbb{R}^d \rightarrow \mathbb{R}^m$ , and an input certification radius  $R$ , median smoothing aims to find a bound for the median of predictions, as given by

$$\tilde{f}(X) = q_{0.5}(X), \quad (3)$$

where  $q_p(X) = \sup\{y \in \mathbb{R} \mid \mathbb{P}[f(X + \epsilon) \leq y] \leq p\}$  is the quantile function with  $q_{0.5}$  indicating the median and  $\epsilon \sim N(0, \sigma^2 I)$ . Then, the certified bounds are as follows for  $\|r\|_2 \leq R$ :

$$q_{\Phi(-\frac{R}{\sigma})}(X) \leq \tilde{f}(X + r) \leq q_{\Phi(\frac{R}{\sigma})}(X), \quad (4)$$

In simple words, with certification, we ensure that if an input to the smoothed predictor is perturbed within a radius  $R$ , the smoothed output remains within a certified bound. The sigma parameter, being a hyperparameter, is not tied to  $R$  and can be adjusted according to the specific needs of different applications. In the extreme case of  $\sigma = 0$ , the output aligns closely with the original predictor, yielding wide bounds. As sigma increases, the influence of randomness becomes more pronounced, causing the certified bounds to tighten, albeit with more smoothed / less accurate predictions. In the utmost scenario of  $\sigma = \infty$ , the smoothed predictor consistently predicts the same values, achieving the tightest possible bounds. The impact of this choice will be demonstrated in the experiments section.

### 3.2 Certified Trajectory Prediction

Pedestrian trajectory prediction tackles a regression task with sequences as inputs and outputs. The location of an agent at any timestep  $t$  is represented by his/her xy-coordinates  $(x_t, y_t)$ . Given an observation sequence for  $T_{obs}$  timesteps as  $X = (x_{-T_{obs}+1}, y_{-T_{obs}+1}, \dots, x_0, y_0)$ , the aim is to predict the next  $T_{pred}$  positions  $g(X) = (x_1, y_1, \dots, x_{T_{pred}}, y_{T_{pred}})$ . Notably, the trajectory predictor  $g$  can be constructed as a function mapping  $\mathbb{R}^{2T_{obs}} \rightarrow \mathbb{R}^{2T_{pred}}$ , making it amenable for certification purposes with  $d = 2T_{obs}$  and  $m = 2T_{pred}$ .

Prior to discussing certification bounds, we introduce our denoiser  $h$ . The denoised smoothing technique combines a classifier with a denoiser  $h$ , by first passing perturbed inputs through the denoiser to preprocess them before being fed into the model. Extending this technique to trajectory prediction, we integrate our predictor  $g$  with  $h$ , making  $f(X) = g(h(X))$ . The denoiser surpasses the randomness before feeding the data to the predictor, facilitating the derivation of tighter certified bounds for  $f$ . In an optimal scenario, where the denoiser exhibits high efficacy ( $h(X + \epsilon) \approx X$ ), we obtain pseudo-clean data for  $g$ , leading to prediction performance closely resembling that of original data. In instances where the denoiser deviates from the ideal, signal denoising still occurs. We utilize the Wiener filter [43] as our denoiser, because of its compatibility with the frequency domain, aligning well with the characteristics of our trajectory data. Note that in experiments without a denoiser, we define the denoiser as the identity function, denoted as  $h = I$ .

As mentioned in [Section 3.1](#), to establish certified bounds in case of mean aggregation for the multi-output human trajectory predictor with  $m = 2T_{pred}$  outputs, one needs to have  $l_j$ 's and  $u_j$ 's. However, inherent to trajectory prediction is the absence of these upper and lower bounds due to the unrestricted spatial nature of the predicted locations. To

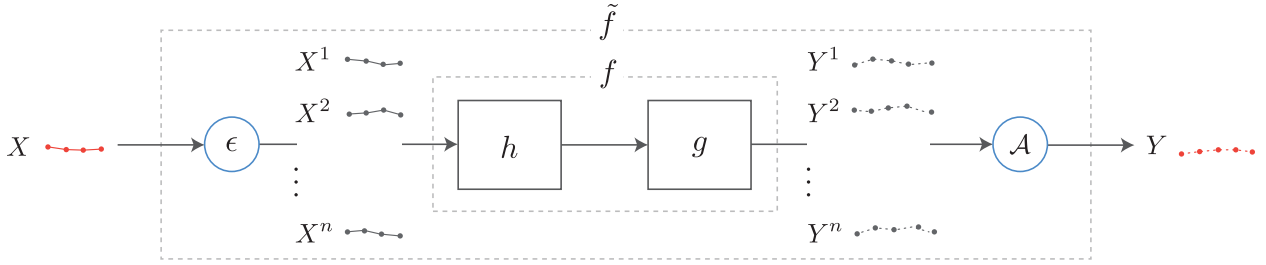


Figure 2: An outline of the proposed smoothed trajectory predictor:  $n$  different randomized input observations  $X^i$  are created by adding randomness  $\epsilon$  to the original one. The denoiser  $h$  processes these samples  $X^i$ , which are then fed into the trajectory predictor  $g$  to make the outputs  $Y^i$ . Applying an aggregation function  $\mathcal{A}$  (median or mean) on these  $Y^i$ , the final smoothed prediction  $Y$  is derived.

address this for our certification equations, we propose adaptive clamping. The process involves computing the predictions given all  $X$  in the training dataset. By determining the maximum and minimum values from these computations, we establish  $l_j = \min_X f_j(X)$  and  $u_j = \max_X f_j(X)$ . However, these bounds are not guaranteed; in other words, with new samples, the predictor may predict outside these estimated bounds, preventing the derivation of certification bounds using the previous equations. To address that, all coordinates of the predicted trajectories  $f_j(X)$  are clamped with  $\min(u_j, \max(l_j, \cdot))$  operator to ensure conformity within the specified range. In the case of median smoothing, these bounds are not required, and we compute the median for each timestep independently.

Finally, it is important to note that recent trajectory prediction models predict multi-modal outputs in order to cover the possible distributions. We consider this property into our design, providing the certified bounds for the best sample out of  $k$  samples (closest to the ground truth) for multi-modal trajectory predictors.

### 3.3 Overview and the algorithm

Figure 2 provides an overview of our approach. Initially, we acquire  $n$  samples from  $\epsilon \sim N(0, \sigma^2 I)$ , adding them to input  $X$  to get  $X^1, \dots, X^n$ . These samples serve dual purposes: for deriving both lower and upper bounds and for smoothing. They are then processed by our denoiser  $h$ . The certified bounds for  $\tilde{f}(X) = \mathcal{A}(g(h(X + \epsilon)))$  are computed according to Equation (2) and Equation (4). Note that  $\mathcal{A}$  represents the aggregation function (either median or mean) applied to  $Y^1, \dots, Y^n$  to yield the final smoothed prediction  $Y$ . The full algorithm is in Algorithm 1.

## 4 Experiments

### 4.1 Datasets and Baselines

**Datasets:** ETH [34], UCY [28], and WildTrack [13] are well-established datasets containing annotations of human positions in crowded environments. We utilize the Trajnet++ [26] benchmark, which provides a fixed data split and unified pre-processing for these datasets. We used the common input and output length for this dataset with  $T_{Obs} = 9$  and  $T_{Pred} = 12$ .

Our experiments involve the following state-of-the-art trajectory predictors:

- **Directional-Pooling (D-Pool) [26]:** D-Pool utilizes relative positions and velocities to learn trajectory features, subsequently pooling these features to capture social interactions. D-Pool is chosen as a baseline due to its demonstrated proficiency in collision avoidance.
- **AutoBot [20]:** Proposes an equivariant feature learning to learn joint distribution of trajectories using multi-head attention blocks.
- **EqMotion [45]:** It is a recent trajectory prediction method appearing at the top of leaderboards. It introduces an efficient equivariant motion prediction model, ensuring motion equivariance and interaction invariance.

Note that while  $\epsilon$  has a Gaussian distribution, the certified bounds are valid for any noise distribution within the radius  $R$ .

---

**Algorithm 1** Smoothed Trajectory Prediction and its Certified Bounds
 

---

```

1: Input: Input trajectory  $X$ , number of Monte-Carlo samples  $n$ , number of predictions  $k$ , aggregation operator  $\mathcal{A}$ ,
   trajectory predictor  $g$ , denoiser  $h$ , certification radius  $R$ , hyperparameter  $\sigma$ , lower bounds  $\{l_j\}$ , upper bounds  $\{u_j\}$ 
2: Output: Certified trajectory prediction  $\tilde{f}(X)$ , the certified bounds
3: procedure
4:   Initialize an empty list  $arr$  to store predictions
5:   for  $i = 1$  to  $n$  do
6:      $\epsilon^i \sim \mathcal{N}(0, \sigma^2 I)$  ▷ Acquire a sample from the Gaussian distribution
7:      $X^i \leftarrow X + \epsilon^i$  ▷ Generate perturbed inputs
8:      $f(X^i) = g(h(X^i))$  ▷ Process through denoiser  $h$  and predictor  $g$ 
9:     if  $\mathcal{A} == \text{Mean}$  then
10:      Clamp the  $j$ -th coordinate of  $f(\cdot)$  within  $[l_j, u_j]$  ▷ Adaptive clamping
11:    end if
12:    Append best of  $f(X^i)$  to  $arr$  ▷ Certify the best of  $k$  predictions
13:  end for
14:   $Y \leftarrow \mathcal{A}(arr)$  ▷ Aggregate the predictions with point-wise mean or median
15:  if  $\mathcal{A} == \text{Mean}$  then ▷ Bounds for mean
16:    Compute lower bound LB and upper bound UB on  $Y$  from Equation (2), given  $R, \{l_j\}, \{u_j\}$ 
17:  else ▷ Bounds for median
18:    Compute lower bound LB and upper bound UB on  $Y$  from Equation (4), given  $R$ 
19:  end if
20:  return  $Y, \text{LB}, \text{UB}$  ▷ Return prediction and certified bounds
21: end procedure
    
```

---

## 4.2 Metrics

In the experiments, we report the performances in the following metrics:

- **Average / Final Displacement Error (ADE/FDE):** These metrics measure the average/final displacement error between the model predictions and its ground truth values. The reported numbers are in meters.
- **Average / Final Bound half-Diameter (ABD/FBD):** Certification provides a smoothed predicted trajectory along with certified bound around each predicted time-step. In order to assess the certified output bounds, we introduce ABD/FBD. They measure the average/final distance of the farthest points within this bound from the predicted trajectory across all timesteps. The reported values are in meters. For the sake of space, we only report numbers in FBD and put the results on ABD in the appendix.
- **Certified-ADE / Certified-FDE:** The common metrics of ADE/FDE are typically reported under the assumption of perfect inputs, meaning they are calculated without considering the impact of input noise. However, in practical scenarios, various types of input noise can occur, which can significantly alter the performance of prediction models. To address this gap and provide a more realistic assessment of model performance under noisy conditions, we propose the Certified-ADE/Certified-FDE metrics that measure the highest ADE/FDE happening given input deviations. They measure the distance of the farthest point in the certified bounds with the ground truth trajectory. The reported values are in meters. For the sake of space, we report numbers in Certified-FDE and put the results on Certified-ADE in the appendix.
- **Certified Collision Rate (Certified-Col):** Collision has been previously introduced as a metric that quantifies the percentage of collisions between the predicted positions of an agent and the ground truth trajectories of neighboring agents in the scene [26]. Employing our output bounds, we introduce Certified Collision Rate (Certified-Col) of a model as the percentage of examples in which at least one neighboring agent lies within the calculated output bound of the predicted trajectory.

## 4.3 Implementation details

The number of Monte-Carlo samples  $n$  is set to 100 throughout the experiments. We set  $R$  to 0.1, and  $\sigma$  range to 0.08–0.4 for the experiments. Note that since  $\sigma$  serves as a hyperparameter, this specific range has been experimentally selected to ensure the models perform effectively. We used the public codes and the default hyperparameters available for the trajectory prediction baselines.



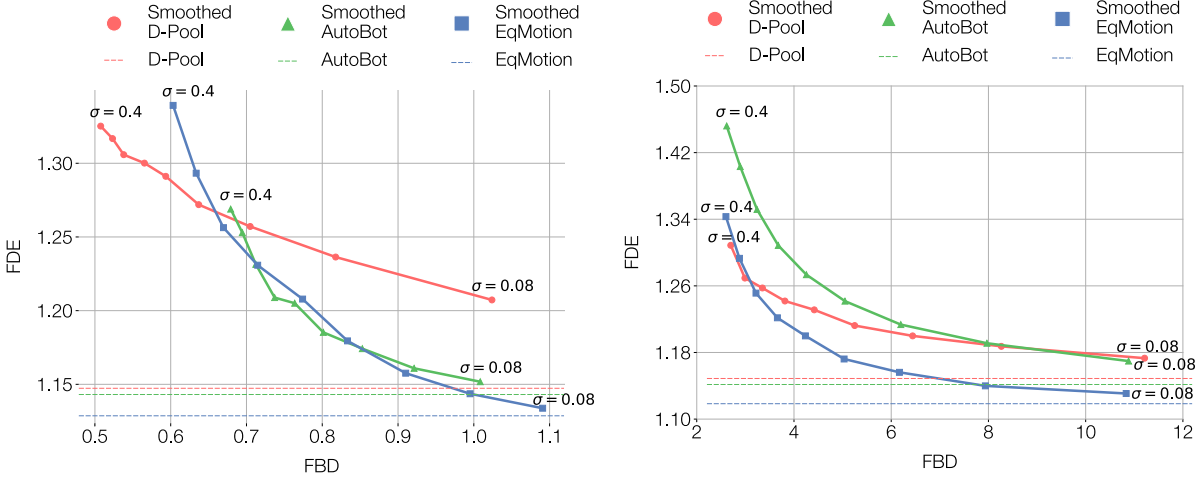


Figure 3: FDE against FBD for *median* aggregation on the left and *mean* aggregation on the right. The results are for different smoothed baselines with two aggregation functions and equally spaced  $\sigma$  within  $[0.08, 0.4]$ . The bottom left indicates the best performance. It shows a trade-off between accuracy (represented in FDE) and robustness (represented as FBD). It also provides a comparison between models’ robustness.

#### 4.4 Results

##### 4.4.1 What is the accuracy and certified bound of different models and is there a trade-off between them?

We initially report the performance of the baselines and their smoothed counterparts utilizing the median aggregation function in the left part of Figure 3. The figure shows the certified bounds of different models against their accuracy. Each point in the curves is an instance of a smoothed model with a different choice of the hyperparameter  $\sigma$ . Therefore, for any desired FDE (resp. FBD), we can select the corresponding FBD (resp. FDE). For instance, given a target FDE of 1.21, the FBD of 0.76, 0.77 and 1.1 are derived for Autobot, EqMotion and D-Pool, respectively. While the original models do not have any bounds, the smoothed models have certified bounds albeit at the expense of a modest increase compared to their original FDE (1% to 6% for different baselines with the smallest  $\sigma$ ).

We also observe that there is a trade-off between accuracy and robustness. By increasing  $\sigma$ , the bounds progressively tighten while the accuracy drops (see Equations (2) and (4)). Note that the choice of the hyperparameter  $\sigma$  allows users to tailor the certification bound according to their preferences. For instance, given a desired FBD of 0.72, we can choose  $\sigma$  of 0.32, 0.28 and 0.16 for Autobot, EqMotion and D-Pool, respectively.

In the right part of Figure 3, we showcase similar curves but utilizing the mean aggregation function. Comparing the two sub-figures highlights that the median aggregator yields considerably smaller bounds compared to the mean aggregator, attributed to the better alignment of the median with the trajectory prediction task. This is probably because trajectory predictors, as regression models, are sensitive to the input noise, producing diverse outputs in response to such noise. As a result, the mean aggregation can become influenced, whereas the median is more robust and less affected. Therefore, we choose median aggregation in the next experiments.

We can also compare the robustness of different baselines by analyzing those curves. Among the baselines, EqMotion and Autobot exhibit comparable high prediction accuracies and low error bounds. While D-Pool exhibits comparable FBDs, it has higher FDE, making it a less accurate prediction model. We have selected EqMotion as our main baseline for subsequent experiments.

In Figure 4, we show qualitative results of EqMotion and smoothed EqMotion. We generate multiple noisy inputs by adding random noise with a magnitude less than 0.1 to an input trajectory and visualize the models’ predictions. As evidenced, the original predictor yields highly variable outputs, however, the smoothed predictor predicts within the certified bounds. It is important to note that the certified bounds are functions of the input; consequently, they are larger in some scenarios and smaller in others (more results in the appendix).

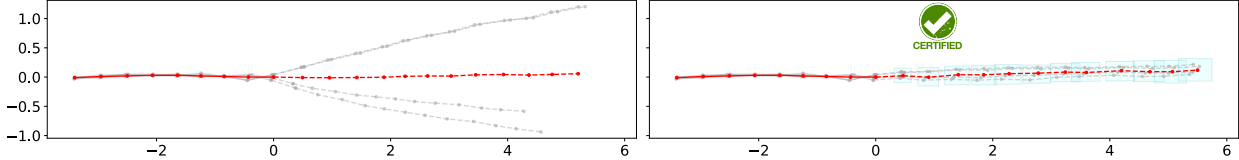


Figure 4: Qualitative results of the original predictor compared with the smoothed predictor. The red trajectories depict clean inputs and the corresponding predictions, and the gray trajectories represent noisy inputs and predictions. The left part showcases the outputs of the original predictor, revealing unbounded predictions. In contrast, the right part demonstrates the outputs of the smoothed predictor, underscoring our ability to certify bounds on predicted outputs.

Table 1: Comparing performance in terms of certified and non-certified metrics. FDE measures the deviation from ground truth and Certified-FDE assesses the prediction considering bounds, *i.e.*, the worst distance between final predicted points for noisy input data and ground truth.

Model	FDE	Certified-FDE	Col	Certified-Col
D-Pool	1.14	-	9.4%	-
Smoothed D-Pool	1.23	2.0	9.0%	49%
AutoBot	1.14	-	8.8%	-
Smoothed AutoBot	1.17	2.05	9.3%	53%
EqMotion	1.12	-	10.1%	-
Smoothed EqMotion	1.14	2.07	10.6%	57%

#### 4.4.2 What is the performance of models in terms of certified metrics?

FDE and collision rates are typically evaluated using perfect inputs, leaving the models’ performances under noisy conditions unknown. However, our Certified-FDE and Certified-Col metrics offer guaranteed performance metrics for any input noise with a magnitude smaller than  $R$ .

We report the performance of models with both certified and non-certified metrics in [Table 1](#). The first observation is that there is a large gap between FDE and certified-FDE, revealing the vulnerability of the models to input noise. This shows the danger of solely relying on non-certified metrics. This analysis also uncovers a noteworthy observation: the model with the minimal FDE (EqMotion) does not align with the model achieving the lowest Certified-FDE (D-Pool), indicating that a more accurate model is not necessarily more robust.

The collision rate, a key metric for evaluating the social understanding of trajectory prediction models, is also reported in [Table 1](#). The results show that D-Pool exhibits the best Certified-Col, and in all baselines, a pronounced difference exists between Certified-Col and Col. This discrepancy underscores the importance of considering certified collision in safety-critical applications.

#### 4.4.3 Is the smoothed model robust against adversarial attacks and real-world imperfect observations?

In this part, we show a scenario to showcase the advantages of the smoothed model over original model. More specifically, we show the robustness of the model in a real-world scenario against adversarial attacks and imperfect observation inputs (*i.e.*, those containing noise). We first investigate the robustness of the model against adversarial attacks by performing PGD attacks [31] on EqMotion and smoothed EqMotion models. We demonstrate a scenario in [Figure 5](#) where the left figure shows the existence of an adversary for EqMotion, which leads to large deviations from the original prediction (more than 2m). However, the right figure shows that conducting PGD attacks on the smoothed model does not lead to predictions outside the certified bound. We provide a quantitative analysis on this in the appendix.

In order to illustrate the impact of imperfect perception systems on the prediction models, we employ an off-the-shelf joint detection and tracking model [47] to extract observation trajectories from nuScenes [6] dataset. [Figure 5](#) visualizes a real-world scenario with both the extracted observation sequence and ground truth. The left figure shows that the imperfection in the observation influences the prediction of the model leading to a large deviation from the prediction with ground truth observation. This clearly shows that the performance of the model is sensitive to the input noise, making the model unreliable. In contrast, the predictions of the smoothed model for both observations sequences remain within the certified bounds, providing a reliable model.



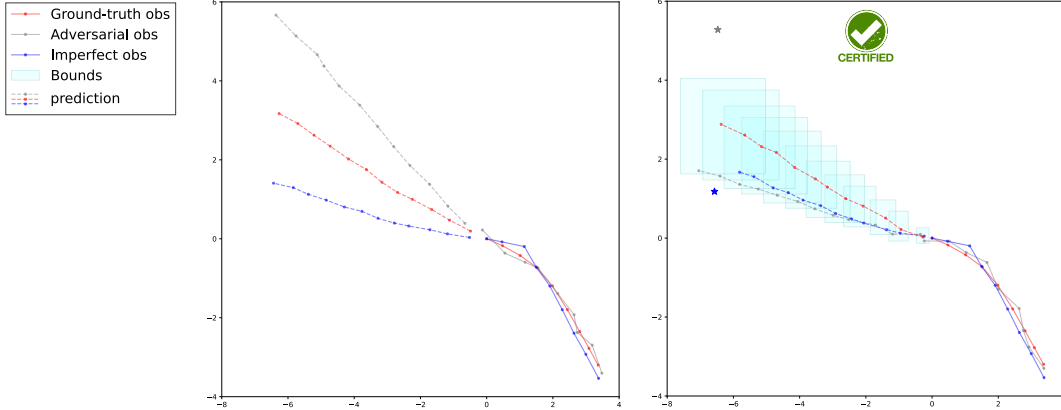


Figure 5: Comparing the performance of the original predictor (on the left) and the smoothed predictor (on the right). The red trajectories depict original observations, the blue trajectories represent predictions with imperfect observations coming from detection and tracking algorithms on real-world data, and the gray ones show the predictions given adversaries. The original predictor outputs change drastically for adversarial and imperfect inputs. In contrast, the smoothed predictor is robust, always predicting within the bounds. To better compare two figures, the final predicted points of the original predictor for the adversarial and imperfect observations were drawn on the right figure with gray and blue stars, respectively.

Table 2: Comparison of output bounds in single vs. multi-agent settings.

Model	FDE	FBD
Single-agent Smoothed EqMotion	1.13	<b>0.99</b>
Multi-agent Smoothed EqMotion	1.13	1.21

Table 3: Comparison of output bounds in single vs. multi-modal settings.

Model	FDE	FBD
Single-modal Smoothed EqMotion	1.13	0.99
Multi-modal Smoothed EqMotion	0.39	<b>0.51</b>

#### 4.4.4 How much are the output bounds affected in multi-modal and multi-agent interaction settings?

Recent trajectory prediction models use the trajectories of all agents in the scene as input in order to account for the interaction between agents resulting in a higher accuracy and predict multi-modal outputs in order to cover the possible distributions. Here, we want to evaluate the impact of these settings on the certified bounds of the models. So far, in our smoothing functions, we applied randomness exclusively to one agent, allowing us to certify the model against perturbations of that agent. This experiment explores the feasibility and impact of expanding certification to all agents by adding randomness to every agent in the scene. **Table 2** shows that with a similar FDE, the single-agent model has a smaller bound size. Indeed, when adding randomness to all agents, the interdependencies between agents make prediction change more, leading to larger bounds for the smoothed models.

For analyzing the performance of our approach in multi-modal settings, we employed the multi-modal EqMotion with 20 predictions for each input similar to [45]. In this setting, we measure FDE considering the closest prediction to the ground truth. We observe in **Table 3** that the multi-modal smoothed EqMotion achieves smaller bounds compared to its single-modal counterpart.

#### 4.4.5 What is the denoiser’s effect in the smoothed model’s performance?

In this part, we aim at comparing the performance of different denoisers, and also investigating the impact of denoiser on the smoothed model’s performance. To evaluate the performance of denoisers, we provide a noisy signal as input to different denoisers and then quantify the residual noise in their output. Since no previous denoiser exists for human trajectories, we tested three established denoising methods for time-series data: the Wiener filter [43] as a statistical

Table 4: Assessing the denoising capability of different denoisers for trajectory data. Noisy trajectory data samples are fed to different denoisers and the magnitude of the remaining noise in their output is reported.

Model	Input Noise=0.08	Input Noise=0.24	Input Noise=0.40
No denoiser	0.08	0.24	0.40
Polynomial	0.08	0.22	0.36
Moving Average	0.07	0.18	0.29
Wiener Filter	<b>0.06</b>	<b>0.16</b>	<b>0.26</b>

Table 5: Comparing FBD with and without denoiser in different settings.

Model	FDE=1.2	FDE=1.3	FDE=1.4
Smoothed EqMotion (w/ denoiser)	1.20	0.96	0.80
Smoothed EqMotion (w denoiser)	<b>0.78</b>	<b>0.65</b>	<b>0.57</b>

approach, a Moving Average filter [35] to filter high-frequency noise, and fitting a 4-th order polynomial as have been used previously to represent human trajectories [4]. The results in Table 4, demonstrate that the Wiener filter outperforms the other approaches in reducing the remaining noise size in different levels of input noise.

We have also studied the effect of removing our denoiser (assigning  $h = J$ ) from our smoothed predictor and demonstrate the results in Table 5. For an equivalent FDE, the denoised smoothed model has a significantly smaller output bound. This shows the effectiveness of the denoiser in reducing the bounds sizes, thus developing a more robust model.

#### 4.5 Computational costs

Randomized smoothing inevitably increases computational costs due to obtaining  $n$  Monte Carlo samples by evaluating the predictor  $n$  times. Nonetheless, this process can be parallelized. We evaluated smoothed EqMotion with  $n = 100$  on one NVIDIA GeForce RTX 3090 and it predicts each sequence of 4.8 seconds length in less than 0.1 seconds, providing the possibility to be used in real-time.

## 5 Conclusions

In this work, we introduced a certified trajectory prediction model that tackles the challenge of guaranteed robustness in trajectory prediction models. Our method is based on denoised smoothing operation where we inject several randomnesses into the input, pass it through a denoiser, and subsequently through a prediction model. Finally, an aggregation operation is employed to derive the smoothed output. We investigated two aggregation functions, mean and median in the context of the trajectory prediction task and introduced certified metrics to measure the performance. Throughout the experiments, we showed the certified bounds for different trajectory prediction baselines using public datasets. We also investigated the relation between accuracy and the bounds. Our experiments showcased the advantages of having guaranteed robustness for the smoothed models once adversarial perturbations or input noise exist. We hope our work paves the way toward more reliable trajectory prediction models.

**Acknowledgments:** The authors would like to thank Brian Sifringer, Taylor Mordan, Ahmad Rahimi, and Yuejiang Liu for their helpful comments. This project was partially funded by Honda R&D Co., Ltd.

## References

- [1] Alahi, A., Goel, K., Ramanathan, V., Robicquet, A., Fei-Fei, L., Savarese, S.: Social lstm: Human trajectory prediction in crowded spaces. In: Proceedings of the IEEE/CVF conference on Computer Vision and Pattern Recognition (CVPR) (2016) 3
- [2] Athalye, A., Carlini, N., Wagner, D.: Obfuscated gradients give a false sense of security: Circumventing defenses to adversarial examples. In: International Conference on Machine Learning (ICML). PMLR (2018) 1
- [3] Bartoli, F., Lisanti, G., Ballan, L., Del Bimbo, A.: Context-aware trajectory prediction. In: International Conference on Pattern Recognition (ICPR). IEEE (2018) 3
- [4] Becker, S., Hug, R., Hübner, W., Arens, M.: An evaluation of trajectory prediction approaches and notes on the trajnet benchmark. arXiv preprint arXiv:1805.07663 (2018) 10

- [5] Bunel, R.R., Turkaslan, I., Torr, P., Kohli, P., Mudigonda, P.K.: A unified view of piecewise linear neural network verification. *Advances in Neural Information Processing Systems (NeurIPS)* **31** (2018) [3](#)
- [6] Caesar, H., Bankiti, V., Lang, A.H., Vora, S., Liong, V.E., Xu, Q., Krishnan, A., Pan, Y., Baldan, G., Beijbom, O.: nuscenes: A multimodal dataset for autonomous driving. *Proceedings of IEEE/CVF Conference on Computer Vision and Pattern Recognition (CVPR)* (2020) [8](#)
- [7] Cao, D., Li, J., Ma, H., Tomizuka, M.: Spectral temporal graph neural network for trajectory prediction. In: *IEEE International Conference on Robotics and Automation (ICRA)*. IEEE (2021) [3](#)
- [8] Cao, X., Gong, N.Z.: Mitigating evasion attacks to deep neural networks via region-based classification. In: *Proceedings of the 33rd Annual Computer Security Applications Conference*. pp. 278–287 (2017) [3](#)
- [9] Cao, Y., Xiao, C., Anandkumar, A., Xu, D., Pavone, M.: Advdo: Realistic adversarial attacks for trajectory prediction. In: *European Conference on Computer Vision (ECCV)*. pp. 36–52. Springer (2022) [1](#), [3](#)
- [10] Cao, Y., Xu, D., Weng, X., Mao, Z., Anandkumar, A., Xiao, C., Pavone, M.: Robust trajectory prediction against adversarial attacks. In: *Conference on Robot Learning (CoRL)*. pp. 128–137. PMLR (2023) [1](#), [3](#)
- [11] Carlini, N., Tramer, F., Dvijotham, K.D., Rice, L., Sun, M., Kolter, J.Z.: (certified!!) adversarial robustness for free! *arXiv preprint arXiv:2206.10550* (2022) [3](#)
- [12] Carlini, N., Wagner, D.: Adversarial examples are not easily detected: Bypassing ten detection methods. In: *Proceedings of the 10th ACM workshop on artificial intelligence and security*. pp. 3–14 (2017) [1](#)
- [13] Chavdarova, T., Baqué, P., Bouquet, S., Maksai, A., Jose, C., Bagautdinov, T.M., Lettry, L., Fua, P., Gool, L.V., Fleuret, F.: Wildtrack: A multi-camera hd dataset for dense unscripted pedestrian detection. *Proceedings of the IEEE/CVF Conference on Computer Vision and Pattern Recognition (CVPR)* (2018) [5](#)
- [14] Chiang, P.y., Curry, M., Abdelkader, A., Kumar, A., Dickerson, J., Goldstein, T.: Detection as regression: Certified object detection with median smoothing. *Advances in Neural Information Processing Systems (NeurIPS)* (2020) [2](#), [3](#)
- [15] Cohen, J., Rosenfeld, E., Kolter, Z.: Certified adversarial robustness via randomized smoothing. In: *International Conference on Machine Learning (ICML)*. pp. 1310–1320. PMLR (2019) [1](#), [2](#), [3](#)
- [16] Dvijotham, K., Stanforth, R., Gowal, S., Mann, T.A., Kohli, P.: A dual approach to scalable verification of deep networks. In: *UAI*. vol. 1, p. 3 (2018) [3](#)
- [17] Ehlers, R.: Formal verification of piece-wise linear feed-forward neural networks. In: *Automated Technology for Verification and Analysis: 15th International Symposium, ATVA 2017, Pune, India, October 3–6, 2017, Proceedings 15*. pp. 269–286. Springer (2017) [3](#)
- [18] Fischetti, M., Jo, J.: Deep neural networks and mixed integer linear optimization. *Constraints* **23**(3), 296–309 (2018) [3](#)
- [19] Franco, L., Placidi, L., Giuliari, F., Hasan, I., Cristani, M., Galasso, F.: Under the hood of transformer networks for trajectory forecasting. *Pattern Recognition* **138**, 109372 (2023) [3](#)
- [20] Girgis, R., Golemo, F., Codevilla, F., Weiss, M., D’Souza, J.A., Kahou, S.E., Heide, F., Pal, C.: Latent variable sequential set transformers for joint multi-agent motion prediction. In: *International Conference on Learning Representations (ICLR)* (2022) [1](#), [3](#), [5](#)
- [21] Giuliari, F., Hasan, I., Cristani, M., Galasso, F.: Transformer networks for trajectory forecasting. In: *2020 25th international conference on pattern recognition (ICPR)*. IEEE (2021) [3](#)
- [22] Huang, X., Kwiatkowska, M., Wang, S., Wu, M.: Safety verification of deep neural networks. In: *Computer Aided Verification: 29th International Conference, CAV 2017, Heidelberg, Germany, July 24–28, 2017, Proceedings, Part I 30*. pp. 3–29. Springer (2017) [3](#)
- [23] Hüllermeier, E., Waegeman, W.: Aleatoric and epistemic uncertainty in machine learning: An introduction to concepts and methods. *Machine Learning* **110**, 457–506 (2021) [3](#)
- [24] Ivanovic, B., Pavone, M.: The trajectron: Probabilistic multi-agent trajectory modeling with dynamic spatiotemporal graphs. In: *Proceedings of the IEEE/CVF International Conference on Computer Vision (ICCV)* (2019) [3](#)
- [25] Jiao, R., Liu, X., Sato, T., Chen, Q.A., Zhu, Q.: Semi-supervised semantics-guided adversarial training for robust trajectory prediction. In: *Proceedings of the IEEE/CVF International Conference on Computer Vision (ICCV)*. pp. 8207–8217 (2023) [1](#), [3](#)
- [26] Kothari, P., Kreiss, S., Alahi, A.: Human trajectory forecasting in crowds: A deep learning perspective. *IEEE Transactions on Intelligent Transportation Systems* (2021) [2](#), [3](#), [5](#), [6](#)

- [27] Kothari, P., Siffringer, B., Alahi, A.: Interpretable social anchors for human trajectory forecasting in crowds. In: Proceedings of the IEEE/CVF Conference on Computer Vision and Pattern Recognition (CVPR) (2021) [3](#)
- [28] Lerner, A., Chrysanthou, Y., Lischinski, D.: Crowds by example. *Comput. Graph. Forum* **26** (2007) [5](#)
- [29] Liu, X., Cheng, M., Zhang, H., Hsieh, C.J.: Towards robust neural networks via random self-ensemble. In: European Conference on Computer Vision (ECCV) (2018) [3](#)
- [30] Liu, Y., Yan, Q., Alahi, A.: Social nce: Contrastive learning of socially-aware motion representations. In: Proceedings of the IEEE/CVF International Conference on Computer Vision (ICCV) (2021) [3](#)
- [31] Madry, A., Makelov, A., Schmidt, L., Tsipras, D., Vladu, A.: Towards deep learning models resistant to adversarial attacks. arXiv preprint arXiv:1706.06083 (2017) [8](#)
- [32] Mohamed, A., Qian, K., Elhoseiny, M., Claudel, C.: Social-stgcnn: A social spatio-temporal graph convolutional neural network for human trajectory prediction. In: Proceedings of the IEEE/CVF Conference on Computer Vision and Pattern Recognition (CVPR). pp. 14424–14432 (2020) [3](#)
- [33] Nikhil, N., Tran Morris, B.: Convolutional neural network for trajectory prediction. In: European Conference on Computer Vision (ECCV) Workshops (2018) [3](#)
- [34] Pellegrini, S., Ess, A., Gool, L.V.: Improving data association by joint modeling of pedestrian trajectories and groupings. In: European Conference on Computer Vision (ECCV). Springer (2010) [5](#)
- [35] Rabiner, L.R., Gold, B.: Theory and application of digital signal processing. Englewood Cliffs: Prentice-Hall (1975) [10](#)
- [36] Saadatnejad, S., Bahari, M., Khorsandi, P., Saneian, M., Moosavi-Dezfooli, S.M., Alahi, A.: Are socially-aware trajectory prediction models really socially-aware? arXiv preprint arXiv:2108.10879 (2021) [1](#), [3](#)
- [37] Saadatnejad, S., Gao, Y., Messaoud, K., Alahi, A.: Social-transmotion: Promptable human trajectory prediction. In: International Conference on Learning Representations (ICLR) (2024) [3](#)
- [38] Salman, H., Sun, M., Yang, G., Kapoor, A., Kolter, J.Z.: Denoised smoothing: A provable defense for pretrained classifiers. *Advances in Neural Information Processing Systems (NeurIPS)* **33**, 21945–21957 (2020) [3](#)
- [39] Shafer, G., Vovk, V.: A tutorial on conformal prediction. *Journal of Machine Learning Research* **9**(3) (2008) [3](#)
- [40] Singh, G., Gehr, T., Mirman, M., Püschel, M., Vechev, M.: Fast and effective robustness certification. *Advances in Neural Information Processing Systems (NeurIPS)* **31** (2018) [3](#)
- [41] Tan, K., Wang, J., Kantaros, Y.: Targeted adversarial attacks against neural network trajectory predictors. In: Learning for Dynamics and Control Conference. pp. 431–444. PMLR (2023) [1](#), [3](#)
- [42] Uesato, J., O’donoghue, B., Kohli, P., Oord, A.: Adversarial risk and the dangers of evaluating against weak attacks. In: International Conference on Machine Learning (ICML). PMLR (2018) [1](#)
- [43] Wiener, N.: Extrapolation, interpolation, and smoothing of stationary time series: with engineering applications. The MIT press (1949) [4](#), [9](#)
- [44] Wong, E., Kolter, Z.: Provable defenses against adversarial examples via the convex outer adversarial polytope. In: International Conference on Machine Learning (ICML). pp. 5286–5295. PMLR (2018) [3](#)
- [45] Xu, C., Tan, R.T., Tan, Y., Chen, S., Wang, Y.G., Wang, X., Wang, Y.: Eqmotion: Equivariant multi-agent motion prediction with invariant interaction reasoning. In: Proceedings of the IEEE/CVF Conference on Computer Vision and Pattern Recognition (CVPR) (2023) [1](#), [3](#), [5](#), [9](#)
- [46] Xu, Y., Chambon, L., Chen, M., Alahi, A., Cord, M., Perez, P., et al.: Towards motion forecasting with real-world perception inputs: Are end-to-end approaches competitive? In: International Conference on Robotics and Automation (ICRA) (2024) [1](#)
- [47] Yin, T., Zhou, X., Krahenbuhl, P.: Center-based 3d object detection and tracking. In: Proceedings of the IEEE/CVF Conference on Computer Vision and Pattern Recognition (CVPR). pp. 11784–11793 (2021) [8](#)
- [48] Zamboni, S., Kefato, Z.T., Girdzijauskas, S., Norén, C., Dal Col, L.: Pedestrian trajectory prediction with convolutional neural networks. *Pattern Recognition* **121**, 108252 (2022) [3](#)
- [49] Zhang, L., Xu, N., Yang, P., Jin, G., Huang, C.C., Zhang, L.: Trajpac: Towards robustness verification of pedestrian trajectory prediction models. In: Proceedings of the IEEE/CVF International Conference on Computer Vision (ICCV). pp. 8327–8339 (2023) [3](#)
- [50] Zhang, Q., Hu, S., Sun, J., Chen, Q.A., Mao, Z.M.: On adversarial robustness of trajectory prediction for autonomous vehicles. In: Proceedings of the IEEE/CVF Conference on Computer Vision and Pattern Recognition (CVPR). pp. 15159–15168 (2022) [1](#), [3](#)

## 6 Appendix

Here, we provide additional content to complement our main paper. This includes an expanded set of qualitative (see [Section 6.1](#)) and quantitative results (see [Section 6.2](#)), followed by an analysis on the bounds with adversarial attacks (see [??](#)). As an additional resource, we have included the pseudo-code for our methodology (see [Section 6.3](#)).

### 6.1 More qualitative results

We show a scenario in [Figure 5](#) of the main paper where we showcase the impact of an adversarial attack and imperfect observation on the performance of the prediction model. Here, we provide more scenarios in [Figure 6](#). These results demonstrate that the models are vulnerable to different input noises, and certification can provide guaranteed robustness.

We have also shown some qualitative results of EqMotion and Smoothed EqMotion on Trajnet++ dataset in [Figure 7](#), underscoring the smoothed predictor’s ability to certify bounds on predicted outputs.

[Figure 8](#) presents qualitative results across varying  $\sigma$  in the smoothed function. It demonstrates the trade-off between accuracy and the bound size. As the sigma value increases, the additive randomness in the smoothing function overwhelms the original input, resulting in a signal whose median aligns closely with the noise median, which is zero. Therefore, the bounds become tighter, but the accuracy drops. Among the various smoothing functions depicted, the one with  $\sigma = 0.16$  appears to maintain a better balance, offering sufficiently tight bounds without significantly compromising accuracy, while the function with  $\sigma = 0.32$  demonstrates relatively lower accuracy.

### 6.2 More quantitative results

In [Section 4](#), we mainly reported in terms of FDE, FBD, and Certified-FDE due to space constraints, and therefore, the outcomes for ADE, ABD, and Certified-ADE are included in [Figure 9](#), [Figure 10](#). We provided the results for various values of  $\sigma$  demonstrating the full spectrum of the results.

### 6.3 Code

In this section, a high-level overview of the methodology is provided via pseudo-code. The function takes an input trajectory  $X$ , along with a predictor  $f$  and denoiser  $h$ , and, based on  $n$ ,  $\sigma$  and the selected aggregation mode, computes the smoothed predictions and certified bounds. For an explanation of the notation used, refer to [Section 3](#).

```
def certified_trajectory_prediction(X, predictor, denoiser, R, n=100,
                                sigma=0.08, l=0.0, u=1.0, aggregation='mean'):

    x_n = X + sigma * torch.randn((n,) + X.shape)
    y_n = predictor(denoiser(x_n))

    cdf = torch.distributions.Normal(0, 1).cdf
    icdf = torch.distributions.Normal(0, 1).icdf

    if aggregation == 'mean':
        y_n = torch.clamp(y_n, min=l, max=u)
        Y = y_n.mean(dim=0)
        eta = sigma * icdf((Y-l)/(u-l))
        LB = l + (u-l) * cdf((eta-R)/sigma)
        UB = l + (u-l) * cdf((eta+R)/sigma)

    elif aggregation == 'median':
        Y = torch.quantile(y_n, 0.5, dim=0)
        LB = torch.quantile(y_n, cdf(-R/sigma), dim=0)
        UB = torch.quantile(y_n, cdf(R/sigma), dim=0)

    return Y, LB, UB
```

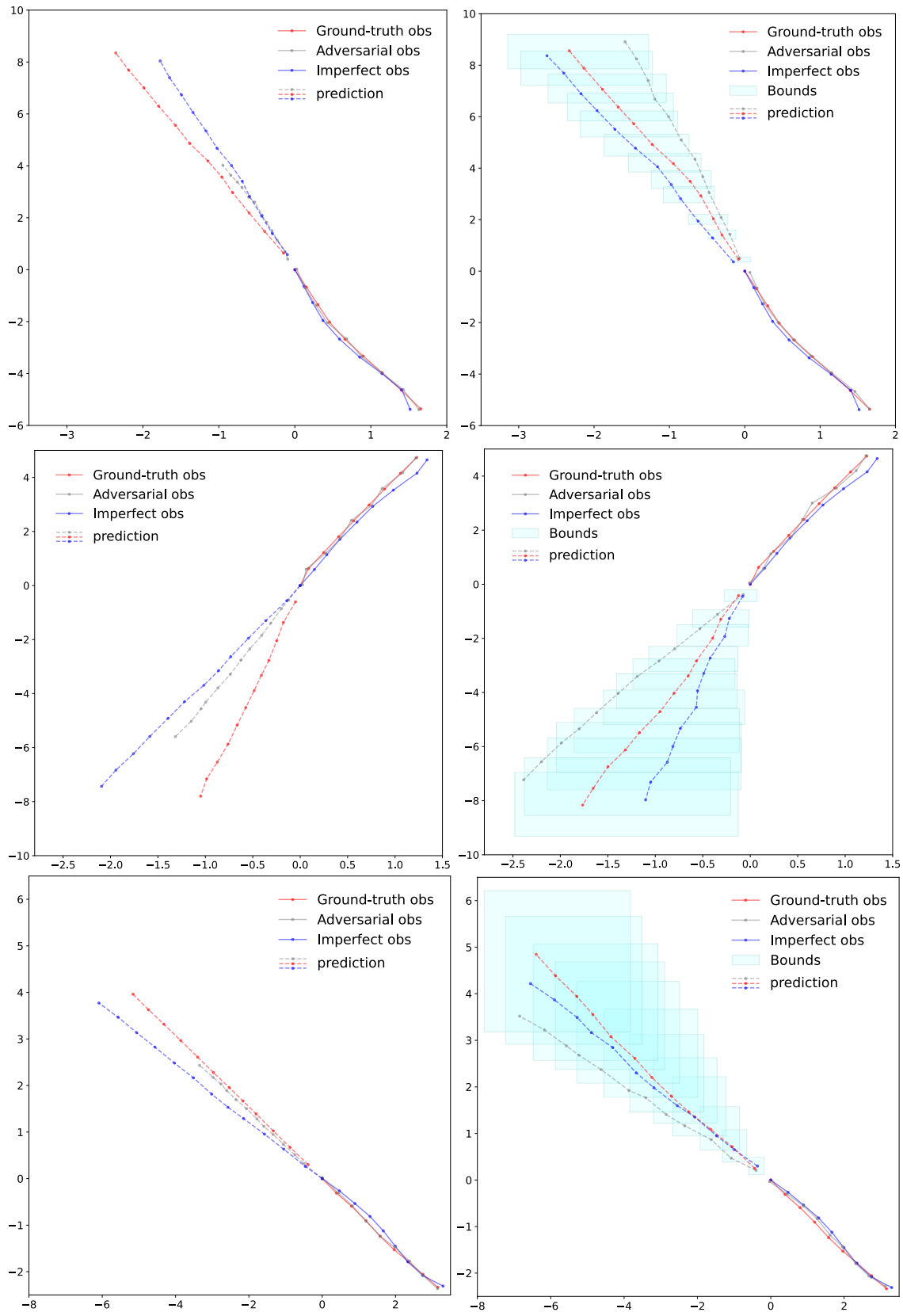


Figure 6: Comparing the performance of the original predictor (on the left) and the smoothed predictor (on the right). The red trajectories depict original observations, the blue trajectories represent predictions with imperfect observations coming from detection and tracking algorithms on real-world data, and the gray ones show the predictions given adversaries.



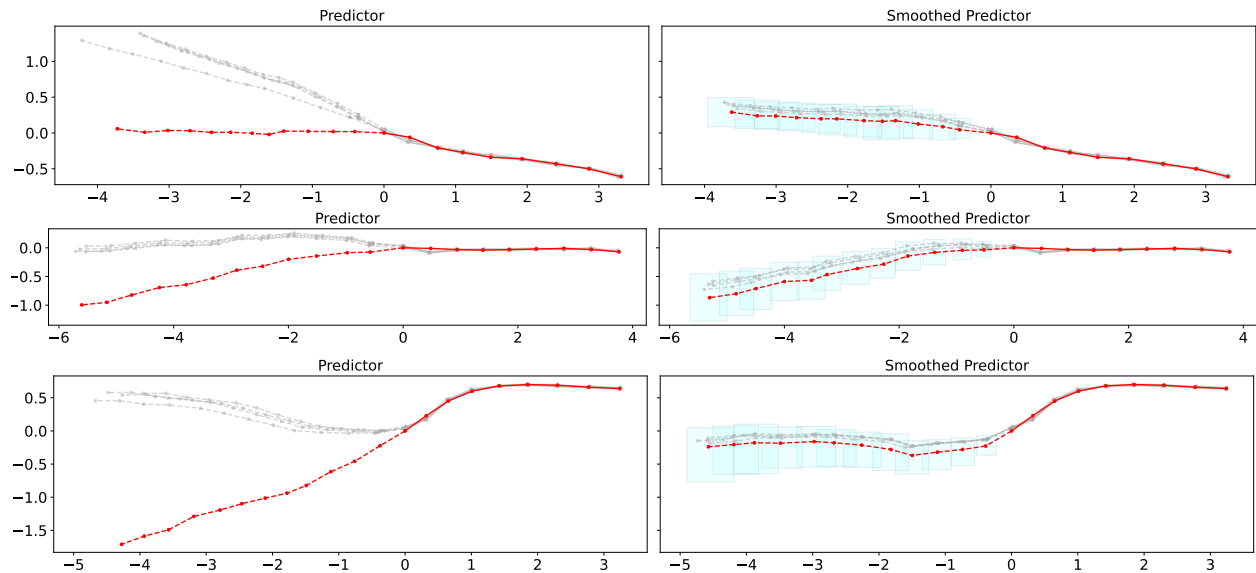


Figure 7: More qualitative results of the original predictor compared with the smoothed predictor. The red trajectories depict original observations and the corresponding predictions, and the gray trajectories represent predictions with noisy inputs. The left part showcases the outputs of the original predictor, revealing unbounded predictions. In contrast, the right part demonstrates the outputs of the smoothed predictor, underscoring our ability to certify bounds on predicted outputs.

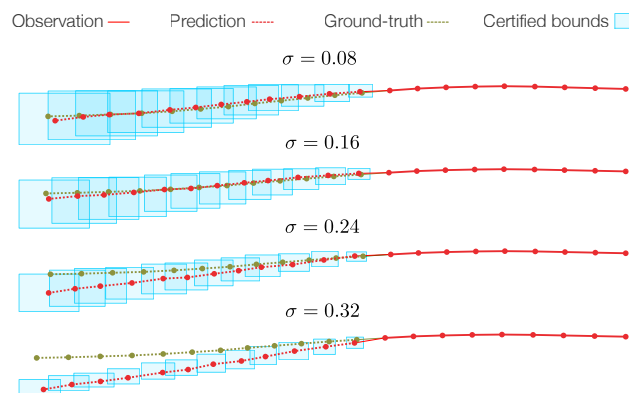


Figure 8: Qualitative results of our model for different values of  $\sigma$ . It shows the outputs of the smoothed EqMotion for one randomly selected data sample in the dataset. The ground-truth predictions are depicted in green, while the observation and the model's predictions are in red. The figure shows that increasing  $\sigma$  tightens the bound at the cost of dropping the accuracy.

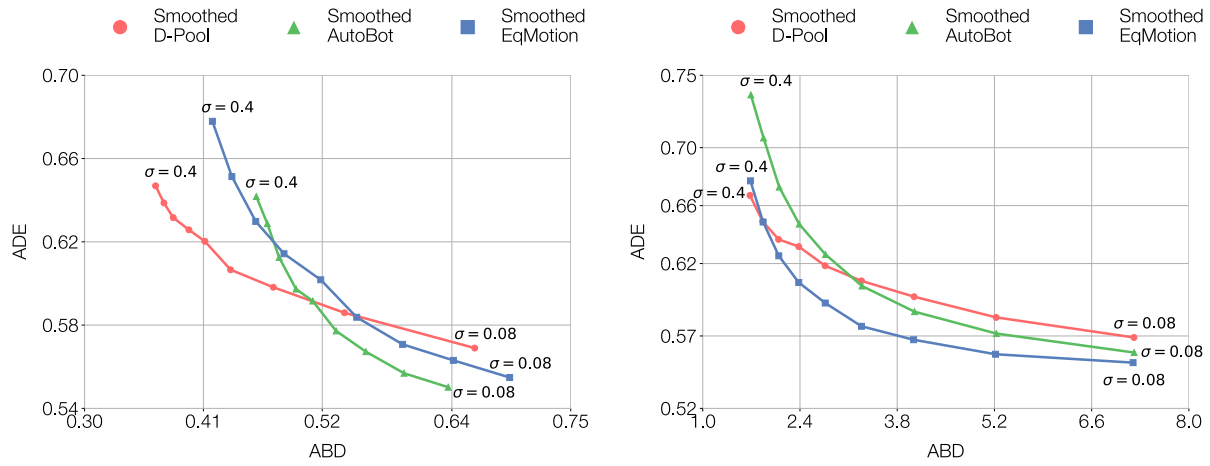


Figure 9: ADE against ABD for median and mean aggregations, respectively. The results are for different smoothed baselines and equally spaced  $\sigma$  within  $[0.08, 0.4]$ . The bottom left indicates the best performance. The conclusions are similar to the main paper.

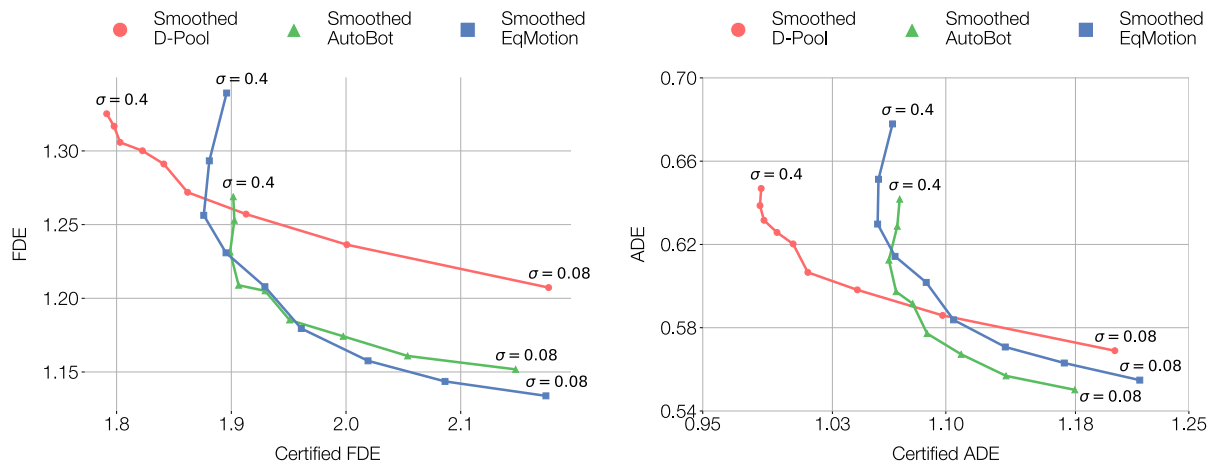


Figure 10: FDE against Certified FDE (on the left) and ADE against Certified ADE (on the right). The results are for different smoothed baselines with median aggregation function and equally spaced  $\sigma$  within  $[0.08, 0.4]$ . The bottom left indicates the best performance. The conclusions are similar to the main paper.